

*This copy is for your personal, non-commercial use only.*

If you wish to distribute this article to others, you can order high-quality copies for your colleagues, clients, or customers by [clicking here](#).

Permission to republish or repurpose articles or portions of articles can be obtained by following the guidelines [here](#).

**The following resources related to this article are available online at [www.sciencemag.org](http://www.sciencemag.org) (this information is current as of June 8, 2010):**

**Updated information and services**, including high-resolution figures, can be found in the online version of this article at:

<http://www.sciencemag.org/cgi/content/full/327/5966/682>

**Supporting Online Material** can be found at:

<http://www.sciencemag.org/cgi/content/full/327/5966/682/DC1>

This article **cites 22 articles**, 6 of which can be accessed for free:

<http://www.sciencemag.org/cgi/content/full/327/5966/682#otherarticles>

This article has been **cited by** 3 articles hosted by HighWire Press; see:

<http://www.sciencemag.org/cgi/content/full/327/5966/682#otherarticles>

This article appears in the following **subject collections**:

Ecology

<http://www.sciencemag.org/cgi/collection/ecology>

The observed pattern of accelerated speciation shows major differences from classic models of adaptive radiation. In these models, phenotypic changes often coincide with genetic isolation of populations in various ecological niches (ecological speciation). Our study demonstrates that the adaptive origin of phenotypic traits that increased colonization ability happened before the radiation of toads. Our macroevolutionary analyses did not identify major changes during the period of accelerated speciation. Yet, as observed in expanding populations, the process of geographic movement may have further driven evolutionary optimization of traits that promoted range expansion (21, 22). We hypothesize that these reciprocal effects have caused the rapid global colonization of bufonids and produced enhanced genetic drift at the expanding frontier, with consequent high levels of population differentiation and speciation (23–25). If so, toads demonstrate an interesting link between macroevolutionary and microevolutionary processes promoting speciation. Because many species radiations now have large distribution ranges, often covering multiple continents (4, 26, 27), evolutionary shifts in traits promoting range-expansion may have significantly contributed to shaping today's ecosystems. Finally, our reconstruction puts the rapid and destructive expansion of the cane toad in Australia into a macroevolutionary context: The origin of this range-

expansion ability appears to be rooted deep in the evolutionary tree of toads and may be a remnant of the period when toads colonized the world.

#### References and Notes

1. S. B. Hedges, S. Kumar, Eds., *The Timetree of Life* (Oxford Univ. Press, New York, 2009).
2. S. Gavrillets, J. B. Losos, *Science* **323**, 732 (2009).
3. B. R. Moore, M. J. Donoghue, *Am. Nat.* **170** (suppl. 2), S28 (2007).
4. R. G. Moyle, C. E. Filardi, C. E. Smith, J. Diamond, *Proc. Natl. Acad. Sci. U.S.A.* **106**, 1863 (2009).
5. F. Bossuyt et al., *Science* **306**, 479 (2004).
6. R. A. Roff, D. J. Fairbairn, in *Dispersal*, E. D. J. Colbert, A. A. Dhondt, J. D. Nichols, Eds. (Oxford Univ. Press, New York, 2001), pp. 191–202.
7. G. Léotard et al., *PLoS ONE* **4**, e5377 (2009).
8. J. B. Pramuk, T. Robertson, J. W. Sites, B. P. Noonan, *Glob. Ecol. Biogeogr.* **17**, 72 (2007).
9. S. Garnica, M. Weiß, B. Oertel, J. Ammirati, F. Oberwinkler, *BMC Evol. Biol.* **9**, 1 (2009).
10. J. A. Pounds, M. L. Crump, *Conserv. Biol.* **8**, 72 (1994).
11. B. L. Phillips, G. P. Brown, M. Greenlees, J. K. Webb, R. Shine, *Austral Ecol.* **32**, 169 (2007).
12. See supporting material on Science Online.
13. W. D. Schmid, *Ecology* **46**, 261 (1965).
14. B. L. Phillips, R. Shine, *Anim. Conserv.* **8**, 407 (2005).
15. R. C. Toledo, C. Jared, *Comp. Biochem. Physiol. A* **105**, 593 (1993).
16. H. R. da Silva, J. R. Mendelson, *Herpetologica* **55**, 114 (1999).
17. P. J. Bentley, *Science* **152**, 619 (1966).
18. H. Szarski, in *Evolution in the Genus Bufo*, W. F. Blair, Ed. (Univ. of Texas Press, Austin, 1972), pp. 71–82.
19. G. Thibaudeau, R. Altig, in *Tadpoles: The Biology of Anuran Larvae*, R. W. McDiarmid, R. Altig, Eds. (Univ. of Chicago Press, Chicago, 1999), pp. 295–337.

20. AmphibiaWeb (<http://amphibiaweb.org>, 2008).
21. B. L. Phillips, *Biol. Lett.* **5**, 802 (2009).
22. B. L. Phillips, G. P. Brown, J. M. J. Travis, R. Shine, *Am. Nat.* **172** (suppl. 1), S34 (2008).
23. J. M. J. Travis et al., *Mol. Biol. Evol.* **24**, 2334 (2007).
24. L. Excoffier, N. Ray, *Trends Ecol. Evol.* **23**, 347 (2008).
25. O. Hallatschek, P. Hersen, S. Ramanathan, D. R. Nelson, *Proc. Natl. Acad. Sci. U.S.A.* **104**, 19926 (2007).
26. I. Van Bocxlaer, K. Roelants, S. D. Biju, J. Nagaraju, F. Bossuyt, *PLoS ONE* **1**, e74 (2006).
27. B. P. Noonan, P. T. Chippindale, *Am. Nat.* **168**, 730 (2006).
28. R. H. Ree, B. R. Moore, C. O. Webb, M. J. Donoghue, *Evolution* **59**, 2299 (2005).
29. We thank S. Bogaerts, R. O. de Sá, N. Poyarkov, M. Wilkinson, K. M. Howell, B. Vervust, B. P. Noonan, A. Channing, and J. V. Vindum for tissue samples; R. Verlinde (Vilda), P. Kok, B. Means, and E. Biggi for pictures; R. Ree for advice on Lagrange analyses; and two anonymous reviewers for valuable comments. Supported by the Institute for the Promotion of Innovation through Science and Technology in Flanders (IWT-Vlaanderen; I.V.B.); a postdoctoral fellowship from the Fonds voor Wetenschappelijk Onderzoek-Vlaanderen (F.B., K.R.); and grants FWO 1.5.039.03N, FWO G.0056.03, FWO G.0307.04, VUB OZR834, and ERC 204509 (project TAPAS). Sequences are deposited in GenBank with accession numbers GU183851 to GU183859 and GU226832 to GU226837.

#### Supporting Online Material

[www.sciencemag.org/cgi/content/full/327/5966/679/DC1](http://www.sciencemag.org/cgi/content/full/327/5966/679/DC1)  
Materials and Methods  
Figs. S1 to S12  
Tables S1 to S4  
Data Files  
References

9 September 2009; accepted 8 December 2009  
10.1126/science.1181707

## Flight Orientation Behaviors Promote Optimal Migration Trajectories in High-Flying Insects

Jason W. Chapman,<sup>1\*</sup> Rebecca L. Nesbit,<sup>1,2</sup> Laura E. Burgin,<sup>3,4</sup> Don R. Reynolds,<sup>1,5</sup> Alan D. Smith,<sup>1</sup> Douglas R. Middleton,<sup>3</sup> Jane K. Hill<sup>2</sup>

Many insects undertake long-range seasonal migrations to exploit temporary breeding sites hundreds or thousands of kilometers apart, but the behavioral adaptations that facilitate these movements remain largely unknown. Using entomological radar, we showed that the ability to select seasonally favorable, high-altitude winds is widespread in large day- and night-flying migrants and that insects adopt optimal flight headings that partially correct for crosswind drift, thus maximizing distances traveled. Trajectory analyses show that these behaviors increase migration distances by 40% and decrease the degree of drift from seasonally optimal directions. These flight behaviors match the sophistication of those seen in migrant birds and help explain how high-flying insects migrate successfully between seasonal habitats.

Long-distance transcontinental migrations by animals are well known, but the orientation strategies employed by migrants are poorly understood (1–3). This is particularly true of insects (4), many of which take advantage of airstreams hundreds of meters aloft for rapid transport between seasonal habitats. For example, moths migrate at altitudes where wind speeds greatly exceed the migrants' self-powered airspeeds (5–7), but the extent to which individuals

are able to move in favorable directions, and how this is achieved, is not clear (2, 8). In contrast with nocturnal insects, day-flying migrant butterflies are usually assumed to travel close to the ground where wind speeds are slower than the insects' airspeeds (9), although substantial butterfly migration may also occur at high altitudes (10, 11). However, whether high-flying butterflies are still capable of maintaining seasonally beneficial migration trajectories, as they can at ground level

(12–14), is not known. More important, the consequences of these flight behaviors for promoting successful migration have not been examined. We studied flight behavior in a range of high-altitude migrant Lepidoptera and modeled the effects of these behaviors on migration trajectories.

We analyzed data from vertical-looking entomological radars [VLR (15)] in the United Kingdom from 2000 to 2007 (16). Our VLRS record large-scale wind-borne migrations 150 to 1200 m above the ground (fig. S1), involving billions of insects. We focus on Lepidoptera, which predominate in these VLR data (6, 17, 18). Using radar data for >100,000 individual insects collected from 569 separate mass migration “events” (16) in spring and fall, we examined seasonal distributions of migratory displacements and flight headings of four groups of migratory insects [the noctuid moths *Autographa gamma* and *Noctua pronuba* (6, 17, 18); hawkmoths (Sphingidae); and butterflies (16)], which spend the winter

<sup>1</sup>Plant and Invertebrate Ecology Department, Rothamsted Research, Harpenden, Hertfordshire AL5 2JQ, UK. <sup>2</sup>Department of Biology, University of York, Heslington, York YO10 5YW, UK. <sup>3</sup>Met Office, FitzRoy Road, Exeter EX1 3PB, UK. <sup>4</sup>School of Geography, University of Exeter, Exeter, Devon EX4 8RJ, UK. <sup>5</sup>Natural Resources Institute, University of Greenwich, Chatham, Kent ME4 4TB, UK.

\*To whom correspondence should be addressed. E-mail: [jason.chapman@bbsrc.ac.uk](mailto:jason.chapman@bbsrc.ac.uk)

around the Mediterranean basin and the summer in northern Europe (6, 11, 19).

During spring, the majority of mass migration events were northward (Fig. 1 and table S1). An individual's displacement direction is the net result of the wind vector and the self-propelled flight vector, but in high-altitude insect migrants, it is largely determined by the wind (16). Mean displacement directions were northward in all taxa (Rayleigh tests, *A. gamma*, 354°; *N. pronuba*, 344°; sphingids, 350°; and butterflies, 353°) (table S2 and fig. S2). The migrants usually showed significant common orientation in their flight headings (the direction of the insect's flight with the effect of the wind removed), and the mean heading of each event was nearly always northward (Fig. 1 and table S1) and thus approximately downwind. The overall mean flight headings of all groups were similar to the corresponding

displacement directions and close to north (Rayleigh tests; *A. gamma*, 18°; *N. pronuba*, 331°; sphingids, 319°; and butterflies, 8°) (table S2 and fig. S2). These migrants ( $n = 43,052$  individuals) were therefore engaged in high-altitude wind-borne transport in seasonally favorable northward directions, which was facilitated by prevailing southwesterly winds (fig. S3).

In the fall, migrants ( $n = 58,902$  individuals) again showed seasonally favorable displacement directions, in this case southward (Fig. 1 and table S1). The mean displacements and flight headings of fall migrants were highly directional, and close to due south (Rayleigh tests for displacements and headings; *A. gamma*: 169° and 195°; *N. pronuba*: 174° and 193°; sphingids: 171° and 190°; and butterflies: 152° and 175°, respectively) (table S2 and fig. S2). However, these return migrations to overwintering areas

could not have resulted from a simple reliance on seasonal changes in wind direction, because prevailing fall downwind directions were toward the east (Rayleigh tests; diurnal downwind direction, 90°; nocturnal downwind direction, 110°;  $P < 0.001$  in both cases) (fig. S3). Meteorological cues are not thought to be used to detect tailwinds (6–8), a supposition that suggests that high-flying migrant insects assess their airborne displacement direction with an internal compass.

The flight headings and displacement directions were similar across the four insect groups within each season (fig. S2 and table S1), and we estimate that these flight behaviors added 4 to 6 m/s of the migrants' airspeeds to the wind vector, which considerably increased distances traveled. The moths achieved extremely rapid transport during migration events (fig. S4 and table S1), with mean speeds of ~15 m/s and maximum speeds of >25 m/s (54 and 90 km/hour, respectively), and would be capable of traveling 400 to 700 km during 8 hours' flight. However, migrants could improve the directedness of their wind-borne displacements if they bias their headings to correct for crosswind drift (20) from their seasonally advantageous preferred compass direction [the "preferred inherited direction" (PID) (6), which we assume is north in spring and south in fall]. During migration events when crosswind drift was relatively minor (i.e., the difference between the displacement direction and the PID was <20°), we found that the mean correction angles (16) of migrants were also small (ranging from -4° to +9°), and distributions were not significantly different from 0° (Fig. 2 and table S3). However, when the drift angle was large (>20°), migrants showed larger corrections (Fig. 2) that were significantly different from 0° (test for a circular mean against a specified alternative;  $P < 0.001$  in all cases except spring-generation sphingids) (table S3).

These data show that high-flying migrants do not simply fly downwind. Rather, when migratory tracks drift >20° from the seasonal PID, migrants take up headings that are significantly biased toward their PID, i.e., they correct for crosswind drift. These correction angles increased in magnitude as the degree of drift away from the PID increased (linear regressions of correction angle on drift angle; spring:  $r^2 = 0.16$ ,  $F_{1,130} = 25.1$ ,  $P < 0.0001$ ; fall:  $r^2 = 0.32$ ,  $F_{1,178} = 86.6$ ,  $P < 0.0001$ ) (fig. S5). The regression slopes were significantly less than one, which implied that the insects showed partial correction [rather than full compensation typical of birds (20)], resulting in higher displacement speeds because a greater component of the organism's airspeed is directed downwind. Furthermore, the mean flight altitude of *A. gamma* was not significantly different from the mean altitude of maximum wind speed [means ( $\pm 1$  SEM) of  $425 \pm 18$  m and  $431 \pm 22$  m, respectively; paired  $t$  test:  $t_{130} = 0.25$ ,  $P = 0.804$ ] (fig. S6), but was significantly different from the mean

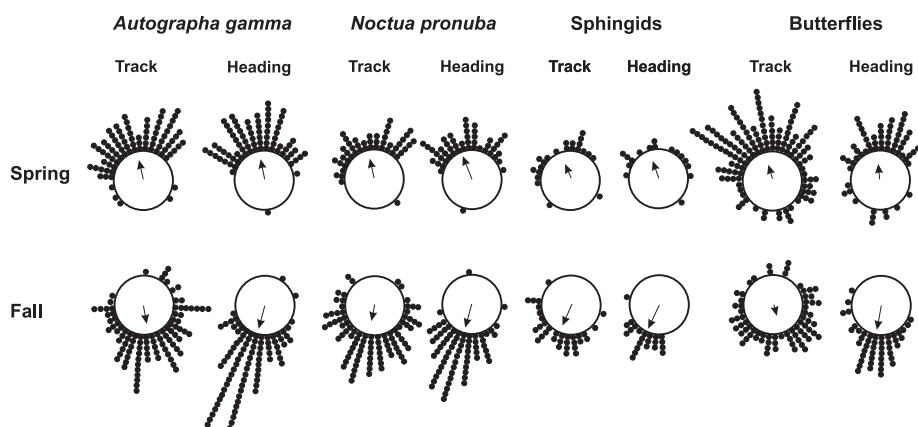


**Fig. 1.** Circular histograms of directional data for high-altitude migration events of four Lepidoptera taxa during spring and fall 2000–2007. Small black circles on the periphery of the large circles represent the mean direction of each migration event. The bearing of the solid black arrows indicates the mean displacement direction (track), or the mean heading, of the migration events, and arrow length is proportional to the degree of clustering of the data set about the mean (the  $r$  value).

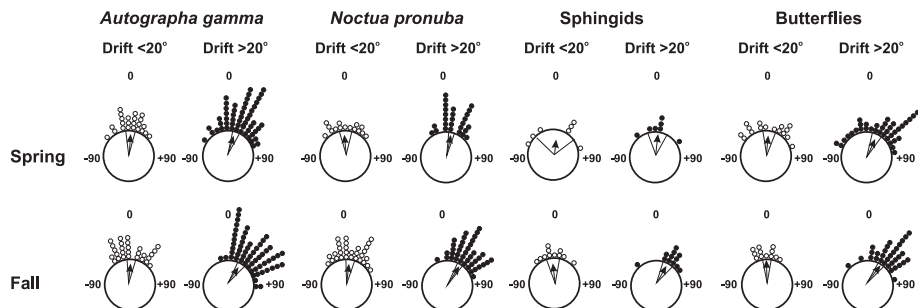


**Fig. 2.** Distributions of correction angles of four insect taxa in spring (top row) and fall (bottom row). A correction angle (small circles at periphery) of 0° indicates that the mean heading of migrants was identical to the mean displacement direction. Positive values (clockwise from 0°) indicate that migrants partially corrected for wind drift by heading in a direction closer toward their PID than their current displacement direction. Conversely, negative values (counterclockwise from 0°) indicate orientation away from the PID. Migration events where the mean displacement direction was close to the seasonal PID (drift angles of <20°) are plotted and analyzed separately from those events where the displacement direction was further from the PID (drift angles of >20°). The arrows and solid lines indicate the mean sample vector and its 95% confidence interval. The figure shows that migrant Lepidoptera partially correct for wind drift when their displacement directions are >20° from their preferred migratory direction.

altitude of most favorable wind direction ( $561 \pm 32$  m) and warmest temperature ( $208 \pm 13$  m). Thus, *A. gamma* moths migrated at high altitudes (fig. S1) and selected the fastest airstreams; migratory flight near the ground was rare [supporting online material (SOM) text].

To evaluate the effect of these observed flight behaviors on migration trajectories, we modeled the flight pathways of migrants using the U.K. Meteorological Office's atmospheric dispersion model NAME (16), which simulates the transport of wind-borne particles. We ran two simulations, assuming migrants either were inert particles passively transported downwind or had *A. gamma*-like flight behavior (and thus were modeled with an additional flight vector of 5 m/s toward their actual heading on each night and were constrained to the altitude of the fastest winds). By contrast, the inert particles were released at the same altitude as moths, but allowed to disperse stochastically throughout the boundary layer. Model simulations of 100 inert particles, or 100 moths, were run for 30 nights in fall 2003 and 2006 when mass return migrations of *A. gamma* occurred (table S4).

The addition of these two simple behavioral rules to the model had a considerable impact on migration trajectories (Fig. 3). The mean displacement directions of inert particle and moth trajectories were significantly different (test for a common mean direction; particles =  $125^\circ$ , moths =  $148^\circ$ ,  $Y = 7.67$ ,  $n = 30$ ,  $P = 0.0056$ ). Furthermore, the end points of the moth trajectories were significantly closer to the fall PID ( $180^\circ$ ) than were the inert particle trajectories [mean drift angles ( $\pm 1$  SEM) of  $35.0^\circ \pm 4.5^\circ$ , and  $57.8^\circ \pm 5.6^\circ$ , respectively; paired  $t$  test:  $t_{29} = 8.2$ ,  $P < 0.0001$ ] (fig. S7 and table S4), which indicated that moth flight headings partially corrected for crosswind drift (by an average of  $22.8^\circ \pm 2.8^\circ$  compared with the inert particles). The moths traveled an additional  $97.8 \pm 5.4$  km during each 8-hour simulation, 40% farther than inert particles (mean distances of 311.3 km and 213.4 km, respectively; paired  $t$  test:  $t_{29} = 18.3$ ,  $P < 0.0001$ ) (fig. S8 and table S4). The distribution of moths showed a significantly lower scatter in the end point of the trajectories compared with inert particles, both in terms of their displacement direction (paired  $t$  test comparing

the standard deviations of the direction:  $t_{29} = 8.9$ ,  $P < 0.0001$ ) and the distance traveled (paired  $t$  test comparing the standard deviations of the distance:  $t_{29} = 6.8$ ,  $P < 0.0001$ ). Thus, the selection of beneficial flight headings and altitudes increases the directedness of the trajectory and distance traveled, while simultaneously reducing the dispersion of the migrants.

The flight behaviors we examined allow insect migrants to utilize fast seasonally favorable tailwinds to maximize the distances traveled. The mechanisms for maximizing migration distance in favorable directions have presumably evolved because most insect migrants have very short migration "windows" (6). In this respect, insects are analogous to Arctic-breeding shorebirds, which also select the fastest high-altitude winds (21), but differ from nocturnal passerine migrants, which select the most favorably directed winds (22); the resulting insect migration speeds are, in fact, considerably faster than those achieved by passerines (2). The relative contribution of different flight behaviors for promoting successful migration during, for example, different weather patterns and in different species needs more

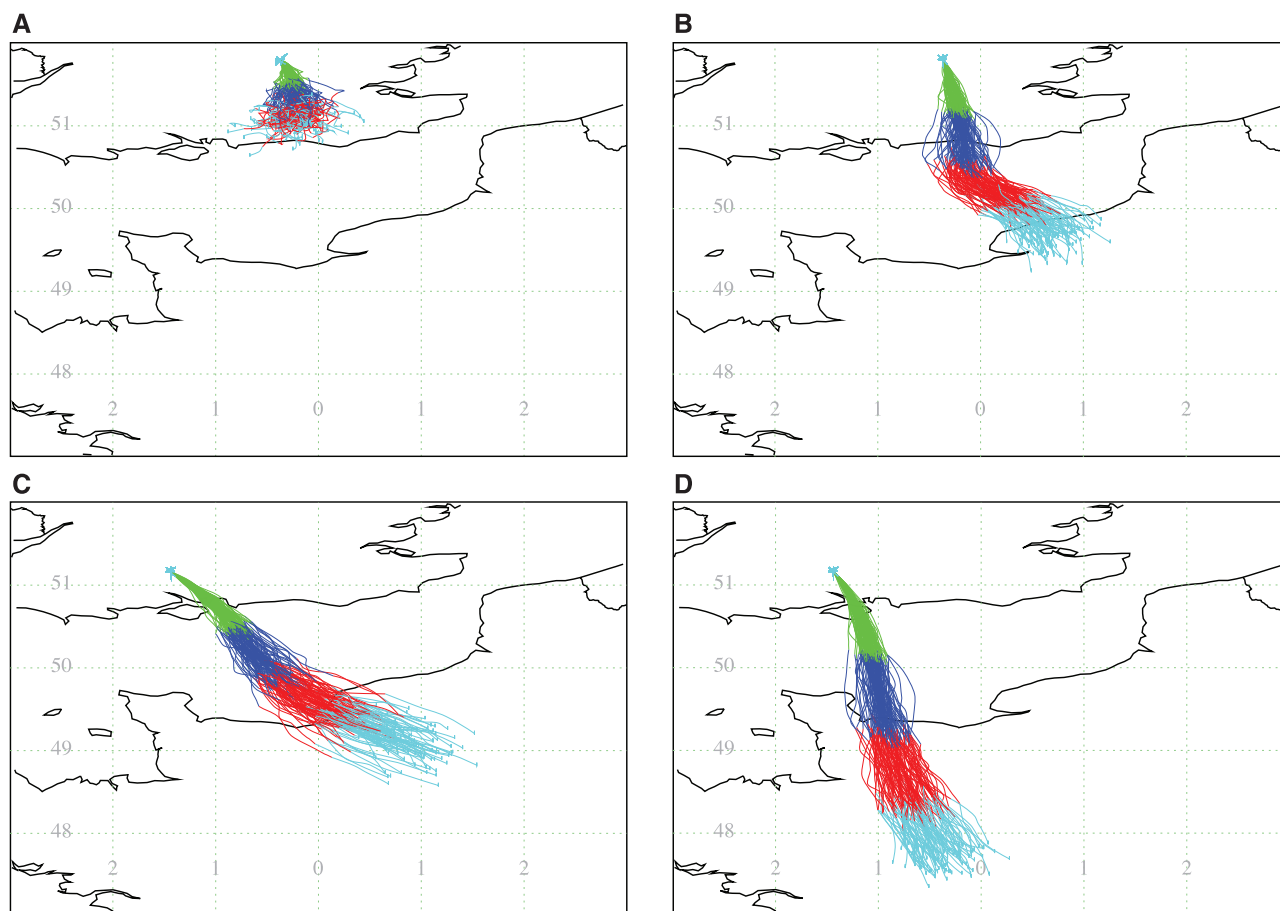


**Fig. 3.** Simulated 8-hour migration trajectories for 100 inert particles and 100 noctuid moths released from two radar sites in southern England; (A and B) Rothamsted, Hertfordshire, on 5 August 2006; (C and D) Chilbolton, Hampshire, on 10 August 2006. The coastlines of southern England and northern France and lines of latitude and longitude are shown. Different colors represent successive 2-hour sections of the trajectory from 20:00 to

04:00 UT. (Left) Trajectories for inert particles, (right) trajectories for moths. (A and B) The considerable effect that moth flight behavior can have on the distance covered [250.0 km in (B) compared with 90.3 km in (A), an increase of 159.7 km]. (C and D) The effect of flight heading on the direction of the trajectory ( $169.0^\circ$  in moths compared with  $144.8^\circ$  in particles, i.e., moth trajectories were  $24.2^\circ$  closer to the seasonally preferred direction of  $180^\circ$ ).

study, but our results imply that many insects may be capable of moving between winter- and summer-breeding sites (~2000 km) in just three or four successive 8-hour migratory flights. These insect migrants are clearly very successful: We estimate that at least 2.3 billion individuals were involved in the high-altitude mass migrations recorded between 2000 and 2007, with ~1.5 times as many individuals involved in fall return migrations as in spring influxes (SOM text). Considering that many migrant insects are important agricultural pests and that the frequency of insect migration to northern latitudes, associated with climate change, is increasing (19, 23), our ability to understand and predict migration strategies will become progressively more important.

#### References and Notes

1. T. Alerstam, *Science* **313**, 791 (2006).
2. S. Åkesson, A. Hedenström, *Bioscience* **57**, 123 (2007).
3. K. Aarestrup *et al.*, *Science* **325**, 1660 (2009).
4. R. A. Holland, M. Wikelski, D. S. Wilcove, *Science* **313**, 794 (2006).
5. C. R. Wood *et al.*, *Int. J. Biometeorol.* **50**, 193 (2006).
6. J. W. Chapman *et al.*, *Curr. Biol.* **18**, 514 (2008).
7. J. W. Chapman *et al.*, *Curr. Biol.* **18**, R908 (2008).
8. R. T. Cardé, *Curr. Biol.* **18**, R472 (2008).
9. R. B. Srygley, R. Dudley, *Integr. Comp. Biol.* **48**, 119 (2008).
10. K. Mikkola, *Entomol. Fenn.* **14**, 15 (2003).
11. C. Stefanescu, M. Alarcón, A. Ávila, *J. Anim. Ecol.* **76**, 888 (2007).
12. H. Mouritsen, B. J. Frost, *Proc. Natl. Acad. Sci. U.S.A.* **99**, 10162 (2002).
13. C. Merlin, R. J. Gegear, S. M. Reppert, *Science* **325**, 1700 (2009).
14. R. L. Nesbit *et al.*, *Anim. Behav.* **78**, 1119 (2009).
15. J. W. Chapman, D. R. Reynolds, A. D. Smith, *Int. J. Pest Manage.* **50**, 225 (2004).
16. Materials and methods are available as supporting material on *Science* Online.
17. J. W. Chapman, D. R. Reynolds, A. D. Smith, E. T. Smith, I. P. Woiod, *Bull. Entomol. Res.* **94**, 123 (2004).
18. C. R. Wood *et al.*, *Bull. Entomol. Res.* **99**, 525 (2009).
19. E. Pollard, J. N. Greatorex-Davies, *Ecol. Lett.* **1**, 77 (1998).
20. M. Green, T. Alerstam, *J. Theor. Biol.* **218**, 485 (2002).
21. M. Green, *Ardea* **92**, 145 (2004).
22. H. Schmaljohann, F. Liechti, B. Bruderer, *Behav. Ecol. Sociobiol.* **63**, 1609 (2009).
23. T. H. Sparks, D. B. Roy, R. L. H. Dennis, *Glob. Change Biol.* **11**, 507 (2005).
24. We thank S. Clark, L. Castle, D. Ladd, P. Clark, G. Hays, J. Phillips, T. Alerstam, D. Thomson, and M. Hort. Rothamsted Research receives grant-aided support from U.K. Biotechnology and Biological Sciences Research Council.

#### Supporting Online Material

www.sciencemag.org/cgi/content/full/327/5966/682/DC1

Materials and Methods

SOM Text

Figs. S1 to S8

Tables S1 to S5

References

7 October 2009; accepted 14 December 2009

10.1126/science.1182990

# Conformational Spread as a Mechanism for Cooperativity in the Bacterial Flagellar Switch

Fan Bai,<sup>1,2\*</sup> Richard W. Branch,<sup>1\*</sup> Dan V. Nicolau Jr.,<sup>3,4\*</sup> Teuta Pilizota,<sup>1,5</sup> Bradley C. Steel,<sup>1</sup> Philip K. Maini,<sup>3,6</sup> Richard M. Berry†<sup>1</sup>

The bacterial flagellar switch that controls the direction of flagellar rotation during chemotaxis has a highly cooperative response. This has previously been understood in terms of the classic two-state, concerted model of allosteric regulation. Here, we used high-resolution optical microscopy to observe switching of single motors and uncover the stochastic multistate nature of the switch. Our observations are in detailed quantitative agreement with a recent general model of allosteric cooperativity that exhibits conformational spread—the stochastic growth and shrinkage of domains of adjacent subunits sharing a particular conformational state. We expect that conformational spread will be important in explaining cooperativity in other large signaling complexes.

The elements of protein signaling networks are often complexes that change their activity in response to binding specific ligands. Multisubunit protein complexes often show cooperativity, with either binding or activity showing a switchlike sigmoidal dependence upon ligand concentration. Cooperativity has classically been understood in terms of the concerted (1) or

sequential (2) models of allosteric regulation, which describe coupling between ligand binding and subunit conformation, and coupling of conformations between different subunits. Both models have deterministic elements. In the concerted model, coupling between subunits is absolute: All subunits switch conformation simultaneously. In the sequential model, coupling between ligand binding and conformation is absolute: When a ligand binds a subunit, that subunit switches. More recently, a mathematical model of the general allosteric scheme proposed by Eigen (3) was constructed in which both types of coupling are probabilistic (4, 5). This model encompasses the classical mechanisms at its limits and introduces the mechanism of conformational spread, with domains of a particular conformational state growing or shrinking faster than ligand binding. Although the classical models have been useful in explaining the regulation of numerous oligomeric proteins (6, 7), conformational spread is a natural extension that will be necessary for

understanding cooperativity in large multimeric protein complexes (4, 8).

The bacterial switch complex in *Escherichia coli* is a large protein ring that controls the direction of rotation of the bacterial flagellar motor (9) (Fig. 1A). The switch response shows a steep sigmoidal relationship between the concentration of the response regulator CheY-P and motor rotational bias (the fraction of time spent rotating in a given direction), contributing to the remarkable gain of the bacterial chemotactic network (10, 11). Binding of CheY-P to FliM protein subunits of the complex is much less cooperative [Hill coefficient <2 (12, 13)] than the switch response [Hill coefficient 10.1 (10)]. In terms of classical allosteric regulation theory, this precludes the sequential model and favors the concerted model, where the binding cooperativity can be less than the response cooperativity (14). Further evidence against the sequential model is that flagellar motors can switch at low temperatures in the absence of CheY (15).

Consistent with the concerted model, the flagellar switch has traditionally been understood in binary terms, with instantaneous switching between stable counterclockwise (CCW) and clockwise (CW) rotation (16–20). However, it is difficult to imagine a mechanism for instantaneous concerted transitions of such a large complex without invoking action at a distance. A conformational spread model of the flagellar switch has been constructed (4) that, in contrast to the two-state concerted model, allows for a multistate switch (Fig. 1, B to D). The directly observable consequence of conformational spread in this system is that switch events should be non-instantaneous with broadly distributed durations due to the biased random walk of conformational spread. Additionally, incomplete switches due to rapid incomplete growth and shrinkage of nucleated domains should be observable as transient speed fluctuations in otherwise stable rotation.

<sup>1</sup>Clarendon Laboratory, Department of Physics, University of Oxford, Parks Road, Oxford OX1 3PU, UK. <sup>2</sup>Nanobiology Laboratories, Graduate School of Frontier Biosciences, Osaka University, 1-3 Yamadaoka, Suita, Osaka, 565-0871 Japan. <sup>3</sup>Centre for Mathematical Biology, Mathematical Institute, University of Oxford, St. Giles, Oxford OX1 3LB, UK. <sup>4</sup>Department of Integrative Biology, Valley Life Sciences Building, University of California–Berkeley, Berkeley, CA 94708, USA. <sup>5</sup>Carl Icahn Laboratory, Princeton University, Washington Road, Princeton, NJ 08544, USA. <sup>6</sup>Oxford Centre for Integrative Systems Biology, Department of Biochemistry, South Parks Road, Oxford OX1 3QU, UK.

\*These authors contributed equally to this work.

†To whom correspondence should be addressed. E-mail: r.berry1@physics.ox.ac.uk